

Changes in Primary Donor Hydrogen-Bonding Interactions in Mutant Reaction Centers from *Rhodobacter sphaeroides*: Identification of the Vibrational Frequencies of All the Conjugated Carbonyl Groups[†]

Tony A. Mattioli,^{*,‡} JoAnn C. Williams,[§] James P. Allen,[§] and Bruno Robert[†]

Section de Biophysique des Protéines et des Membranes, Département de Biologie Cellulaire et Moléculaire, CEA and URA CNRS 1290, C. E. Saclay, 91191 Gif-sur-Yvette cedex, FRANCE, and Department of Chemistry and Biochemistry and the Center for the Study of Early Events in Photosynthesis, Arizona State University, Tempe, Arizona 85287-1604

Received October 26, 1993; Revised Manuscript Received December 20, 1993*

ABSTRACT: Specific changes in the hydrogen-bonding states of the primary donor, P, in reaction centers from *Rhodobacter sphaeroides* bearing mutations near P were determined using near-infrared excited Fourier transform (FT) Raman spectroscopy. This technique, using 1064-nm excitation, provides the preresonantly enhanced vibrational spectrum of P in its reduced state selectively over the contributions of the other reaction center chromophores and protein and yields structural information concerning P and its hydrogen-bonding interactions. The mutations studied were as follows: Leu M160 → His, Leu L131 → His, the D9 double mutant (Leu M160 → His + Leu L131 → His), Phe M197 → His, and His L168 → Phe. These mutations were designed to introduce new, or to break existing, hydrogen bonds to the C₉ and C₂ carbonyl groups of P. On the basis of previous assignments [Mattioli, T. A., Hoffmann, A., Robert, B., Schrader, B., & Lutz, M. (1991) *Biochemistry* 30, 4648–4654], the FT Raman spectra of these mutants show the predicted changes in hydrogen bond interactions of P carbonyl groups with the protein. The results of this study have permitted us to unambiguously identify the C₂ and C₉ carbonyl vibrators of P in *Rb. sphaeroides*. The genetically introduced hydrogen bond interactions are discussed in terms of other physicochemical properties of P including the redox potential and electronic asymmetry in the P⁺ state. It is discussed that changes in protein hydrogen bonding to the conjugated carbonyl groups of P alone are not the sole factor that contributes to the sizable modifications of the P/P⁺ redox midpoint potentials, and that the chemical nature of the hydrogen bond donor plays a significant role in this modification.

The bacterial reaction center (RC)¹ is a specialized, integral membrane protein wherein the primary events of photosynthesis occur. The structural elucidation of reaction centers from two purple photosynthetic bacteria, *Rhodospseudomonas (Rps.) viridis* (Michel *et al.*, 1986) and *Rhodobacter (Rb.) sphaeroides* (Allen *et al.*, 1987; Yeates *et al.*, 1988; El-Kabbani *et al.*, 1991; Ermler *et al.*, 1992) has revealed the specific spatial arrangement of the cofactors that mediate the photoinduced transmembrane charge separation. The RC from *Rb. sphaeroides* 2.4.1 consists of three polypeptides named L, M, and H. The L and M polypeptides noncovalently anchor several cofactors: a pair of excitonically coupled bacteriochlorophyll *a* (BChl *a*) molecules constituting the primary electron donor (P), two monomeric BChl *a* molecules (BChl_L and BChl_M), two bacteriopheophytin *a* molecules (BPhe_L and BPhe_M), two ubiquinone molecules (Q_A and Q_B), a non-heme

iron atom, and a carotenoid molecule. These cofactors (excluding the carotenoid) are arranged in pairs along a pseudo-C₂ symmetry axis which extends from P to the non-heme iron, resulting in two branches called L and M. Excitation of the primary donor by the absorption of light or the trapping of a singlet exciton results in the formation of its first excited electronic singlet state, P^{*}. Subsequent electron transfer from P^{*} to the acceptor, BPhe_L, occurs in ca. 3 ps (Woodbury *et al.*, 1985; Martin *et al.*, 1986; Holzappel *et al.*, 1990) and then to Q_A in ca. 200 ps (Kirmaier *et al.*, 1985).

To address the question of structure–function relationships in the RC, *Rb. sphaeroides* mutants have recently been constructed that are designed to introduce or remove hydrogen bonds on carbonyl groups conjugated to the π -electronic system of the two BChl molecules constituting P (Williams *et al.*, 1992a; Murchison *et al.*, 1993), as listed in Table 1. According to the crystal structures of the *Rps. viridis* (Michel *et al.*, 1986) and *Rb. sphaeroides* RCs (Allen *et al.*, 1987; Yeates *et al.*, 1988; El-kabbani *et al.*, 1991), the primary donor of both species are asymmetrically hydrogen bonded at the level of the carbonyl groups. In *Rb. sphaeroides*, the primary donor appears to be hydrogen bonded only at the C₂ acetyl carbonyl of P_L via the histidine L168 residue; the other acetyl carbonyl and the two C₉ keto carbonyls are proposed not to be engaged in hydrogen bond interactions according to the X-ray structures (Yeates *et al.*, 1988; El-kabbani *et al.*, 1991; Chirino *et al.*, 1994).

Recently, we have reported the FT preresonance Raman spectrum of the primary donor from *Rb. sphaeroides* R 26 RCs. From the selective observation of P alone, well-resolved Raman bands corresponding to the stretching modes of the

[†] Part of this work was supported by Grants GM41300 and GM45902 from the National Institutes of Health. The Center for the Study of Early Events in Photosynthesis is funded by DOE Grant DE-FG-88-ER13969 as a part of the USDA/DOE/NSF Plant Science Centers Program. This is publication no. 183 from the Center for the study of Early Events in Photosynthesis.

* Corresponding author.

[‡] C. E. Saclay.

[§] Arizona State University.

[•] Abstract published in *Advance ACS Abstracts*, February 1, 1994.

¹ Abbreviations: *Rps.*, *Rhodospseudomonas*; *Rb.*, *Rhodobacter*; *Rsp.*, *Rhodospirillum*; RC, reaction center; P, primary electron donor; BChl, bacteriochlorophyll; BPhe, bacteriopheophytin; RR, resonance Raman; NIR, near infrared; FT, Fourier transform; FTRR, Fourier transform (pre)resonance Raman; THF, tetrahydrofuran; Tris, tris(hydroxymethyl)aminomethane; EDTA, (ethylenedinitrilo)tetraacetic acid; LDAO, lauryldimethylamine *N*-oxide.

Table 1: Mutations Designed To Alter Hydrogen Bonds to the Primary Electron Donor in *Rb. sphaeroides*

mutant	change	expected change in hydrogen bond ^a	observed carbonyl ^b frequency			
			WT (cm ⁻¹)	mutant (cm ⁻¹)	Δ^c	ΔH^d
HF(L168)	His L168 → Phe	broken C ₂ =O P _L	1620	1653	+33	0.207
FH(M197)	Phe M197 → His	formed C ₂ =O P _M	1653	1630	-23	0.145
LH(M160)	Leu M160 → His	formed C ₉ =O P _M	1679	1657	-22	0.135
LH(L131)	Leu L131 → His	formed C ₉ =O P _L	1691	1673	-18	0.114

^a Williams *et al.* (1992); Murchison *et al.* (1993). ^b Assignments of wild-type *Rb. sphaeroides* from Mattioli *et al.* (1991). ^c Difference in vibrational frequency of carbonyl vibrator in mutant reaction center as compared to wild type. ^d Estimated hydrogen bond enthalpy from the Badger-type empirical relation given in Zadorozhnyi and Ishchenko (1965).

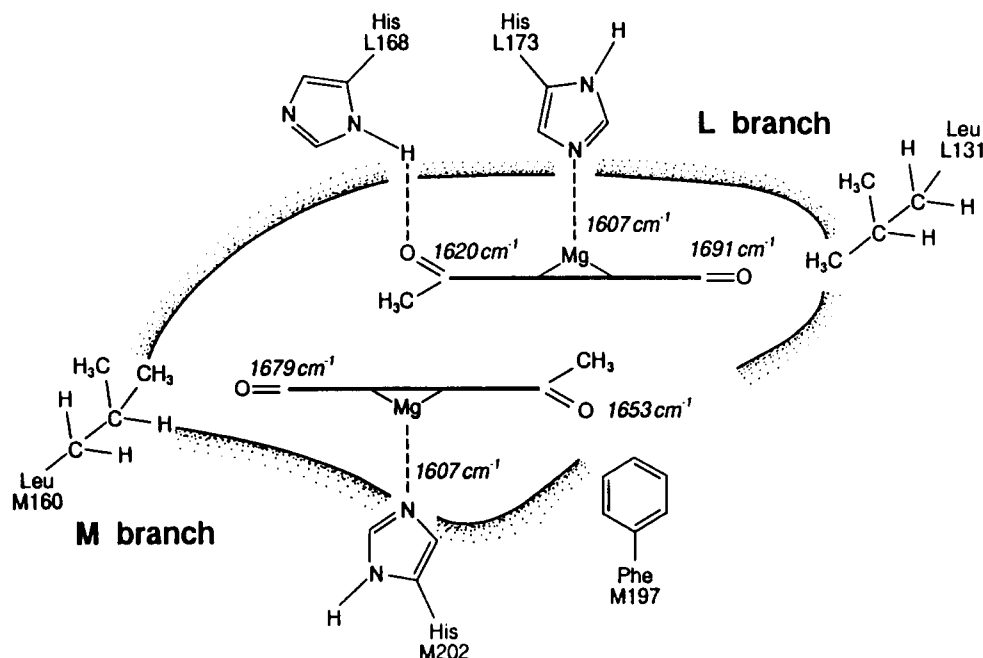


FIGURE 1: Schematic diagram presenting the pigment-protein interaction structural model of the primary donor in *Rb. sphaeroides* and the vibrational frequency assignments of the acetyl and keto carbonyl groups as deduced from the crystal structure and FT Raman spectroscopy (Mattioli *et al.*, 1991). Also shown are the neighboring residues which have been mutated. The vibrational frequency of 1607 cm⁻¹ denotes that of the C₈C_m mode and indicates one axial ligand on the central Mg atom.

four conjugated carbonyl groups of P could be easily and unambiguously observed (Mattioli *et al.*, 1991). On the basis of the observed Raman frequencies and the X-ray crystal structure of *Rb. sphaeroides*, as well as the observed upshift of the C₉ keto carbonyl stretching mode frequency of BChl a upon one-electron oxidation in nonprotic solvent, we have assigned the carbonyl-associated bands in the FT Raman spectrum to the two C₂ and two C₉ carbonyls of P [see Table 1 in Mattioli *et al.* (1991)]. Figure 1 presents the hydrogen bond interaction model for P from *Rb. sphaeroides* as deduced from its FT Raman spectrum and the crystallographic structures. The model is used to evaluate the changes in hydrogen bond interactions of the mutants studied here (Table 1).

Vibrational spectroscopy provides one of the best means of detecting hydrogen bonds. Resonance Raman spectroscopy is a powerful, selective tool in probing pigment-protein interactions, such as hydrogen bonding, in photosynthetic proteins (Lutz, 1984; Lutz & Robert, 1988; Robert, 1990) and their changes upon point mutations. Selective Raman excitation of the primary donor in photosynthetic purple bacterial RCs is now possible using near-infrared excitation and detection (Donohoe *et al.*, 1990; Mattioli *et al.*, 1991, 1993; Shreve *et al.*, 1991; Palaniappan *et al.*, 1992; Wachtveitl *et al.*, 1993). Near-infrared (NIR) Fourier transform Raman spectroscopy utilizes 1064-nm light to excite the Raman spectrum of reaction centers and is highly selective in the

observation of the vibrational spectrum of P and P⁺ via pre- and resonance Raman enhancements of these species, respectively (Mattioli *et al.*, 1991, 1993). Thus, the hydrogen bonding states of the conjugated carbonyls of P are directly ascertainable as are changes in these interactions resulting from mutations (Wachtveitl *et al.*, 1993). As well, the NIR FT Raman technique provides information concerning the localization of the resulting positive charge, or unpaired electron spin density, in the oxidized P⁺ species (Mattioli *et al.*, 1991, 1992a; Wachtveitl *et al.*, 1993) that is complementary to the information obtained by ENDOR techniques [Lendzian *et al.*, 1990; Rautter *et al.*, 1992; reviewed in Lubitz (1991)].

Using FT resonance Raman spectroscopy, we report changes in hydrogen bond interactions for the conjugated carbonyl groups of P in RCs from *Rb. sphaeroides* bearing the following mutations: His L168 → Phe (Murchison *et al.*, 1993), Phe M197 → His (Williams *et al.*, unpublished results), Leu M160 → His, and Leu L131 → His (Williams *et al.*, 1992a) (Table 1). As well, we report changes in the localization of the positive charge as a result of the mutations. From this work and in conjunction with other recent work (Wachtveitl *et al.*, 1993), it has emerged that the chemical nature of the hydrogen bond donor to a C₂ or C₉ carbonyl group of P is important in modifying the redox properties of P.

EXPERIMENTAL PROCEDURES

Mutagenesis, Bacterial Growth, and RC Isolation. A full description of the construction of the mutants, the growth conditions of the mutant bacterial strains, and the isolation of their RCs are found in Williams *et al.* (1992a) and Murchison *et al.* (1993). Isolated RCs were prepared in 15 mM Tris-HCl buffer, pH 8, 1 mM EDTA, and 0.025% LDAO. For all experiments, wild-type RCs were those isolated from the deletion strain complemented with the wild-type genes described in Williams *et al.* (1992a).

Fourier Transform Raman Spectroscopy. The FT Raman spectra of reaction centers were recorded using a Bruker IFS 66 interferometer coupled to a Bruker FRA 106 Raman module as described elsewhere (Mattioli *et al.*, 1991). The excitation source was a diode-pumped Nd:YAG laser delivering ca. 180 mW of 1064-nm radiation. Reaction centers were poised in their P^0 or P^+ states using ascorbate or ferricyanide, respectively. RC samples were contained in a sapphire cell (Schrader *et al.*, 1990) and their spectra recorded at room temperature. Instrumental error is ± 1 cm^{-1} and spectral resolution is at 4 cm^{-1} .

For RC mutants that could not be oxidized by ferricyanide, the P^+ state was photochemically trapped by illumination of the RC sample at room temperature followed by rapid cooling to 77 K. White-light illumination (ca. 1 min) was performed using a tungsten lamp (150 W) whose light was filtered through 5 cm of water to avoid heating. Once frozen, the sample was transferred to a gas-flow cryostat (SMC-TBT, France) in which cold helium gas was circulated, and FT Raman spectra were recorded at 15 K. The low temperature P^+ spectra so obtained were compared to those at 15 K of a nonilluminated RC sample poised in ascorbate under the same experimental and geometric conditions.

RESULTS

Hydrogen Bonding. The effects of hydrogen bonding on chlorophyll carbonyl group vibrations are now well characterized (Lutz, 1984; Lutz & Mäntele, 1991). *In vitro* Raman studies have shown that for BChl *a* the frequency of the C_2 acetyl carbonyl vibrational mode is observed between 1665 (free) and 1620 cm^{-1} (hydrogen bonded), whereas that of the C_9 keto carbonyl may be observed in the 1710–1650- cm^{-1} range (Lutz, 1984); the extent of the downshift reflects the strength of the hydrogen bond. Carbonyl vibrations are also sensitive to unspecific solvent interactions which depend on solvent polarity and polarizability. The observed vibrational frequency of the keto carbonyl of Chl *a* in various solvents of greatly differing polarity, polarizability, dielectric constants, and refractive indices may vary as much as 15 cm^{-1} in the extreme cases (Krawczyk, 1989, and references therein). Thus, frequency shifts of greater than 15 cm^{-1} may be confidently ascribed to changes in hydrogen bond states.

FT Raman Spectrum of the Reduced Primary Donor, P^0

Wild Type. The FT Raman spectrum of reduced wild-type reaction centers from *Rb. sphaeroides* is shown in Figure 2A. This spectrum is identical to that of the carotenoidless R 26 strain; the assignments of the high-frequency bands of P in its reduced state are detailed elsewhere (Mattioli *et al.*, 1991) and are consistent with the X-ray crystal structure (El-Kabbani *et al.*, 1991; Yeates *et al.*, 1988; Chirino *et al.*, 1994) (see model in Figure 1). Briefly, the 1607- cm^{-1} band arises from, predominantly, C_aC_m methine bridge stretching mode contributions. Its observed frequency and narrow bandwidth (ca.

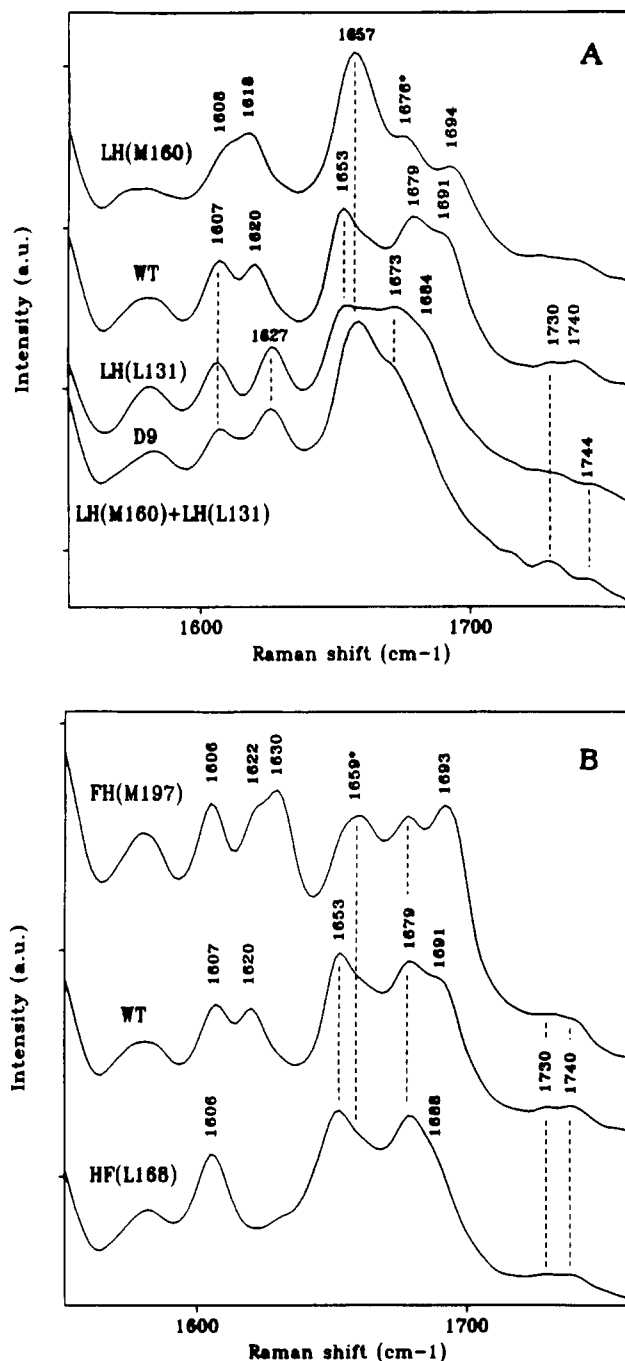


FIGURE 2: Room temperature P^0 FT preresonance Raman spectra of *Rb. sphaeroides* wild type and mutant reaction centers in which the hydrogen bonding states of (A) the C_9 keto carbonyl groups (B) and the C_2 acetyl carbonyls of P have been altered. Reaction centers are poised in their P^0 state, in the presence of ascorbate. The 1676- cm^{-1} band (*) in the LH(M160) spectrum does not arise from P . Excitation was at 1064 nm, with 180 mW of power, 4000 interferograms, and 4- cm^{-1} spectral resolution.

14 cm^{-1} FWHM) indicates that both BChl *a* molecules constituting P possess one axial ligand each; from the X-ray crystal structure of *Rb. sphaeroides* (El-Kabbani *et al.*, 1991; Yeates *et al.*, 1988), these axial ligands are His M200 and His L173. The 1620- cm^{-1} band arises from a C_2 acetyl carbonyl which is involved in a strong hydrogen bond and has been assigned to that of P_L . The 1653- cm^{-1} band arises from a free C_2 acetyl carbonyl and has been assigned to that of P_M . There is a shoulder on the main 1653 cm^{-1} band at ca. 1660 cm^{-1} which is not attributable to P because this component is also observed in the P^+ spectrum and which could arise

from the protein or the accessory BChls (Robert, 1990). The 1679- and 1691- cm^{-1} bands have been assigned to two free C_9 keto carbonyls of the primary donor. The 1691- cm^{-1} band has been specifically assigned to the C_9 keto carbonyl of P_L on the basis that only this frequency (and not that of 1679 cm^{-1}) is consistent with the magnitude of the upshift in frequency of this carbonyl mode upon P^+ formation [see Mattioli *et al.* (1991) for a full discussion].

LH(M160) Mutant. This mutation was designed to introduce a new hydrogen bond on the C_9 keto carbonyl of P_M . According to our model, such a new hydrogen bond would be seen in the FT Raman spectrum of P as a shift of the 1679- cm^{-1} band to lower frequencies. This is observed in Figure 2A where the intense 1679- cm^{-1} band is no longer present and a new band is observed at ca. 1657 cm^{-1} . This new band is very similar in frequency to the 1653- cm^{-1} band making these two bands unresolved. The component corresponding to the 1653- cm^{-1} band in the WT P^0 spectrum is comprised of the large 1657- cm^{-1} band whose integrated area is approximately twice that of the 1653- cm^{-1} band. There is a weak band at 1676 cm^{-1} in the FT Raman spectrum of the LH(M160) mutant cannot be assigned to a carbonyl of the primary donor since this band persists in the P^+ spectrum (see Figure 3A). Thus, we conclude that the 1679- cm^{-1} band has downshifted 22 cm^{-1} to 1657 cm^{-1} consistent with the formation of a new hydrogen bond on a keto carbonyl of P and, specifically, according to our model on the keto carbonyl of P_M . This mutant also displays some minor bandshifts (2–3 cm^{-1}) compared to WT that do not signal new hydrogen bond states but which are probably due to minor variations in the existing interactions.

LH(L131) Mutant. This mutation was designed to introduce a new hydrogen bond on the C_9 keto carbonyl of P_L ; according to the model, we expect the 1691- cm^{-1} band in the WT spectrum to downshift. Comparing the LH(L131) mutant P^0 FT Raman spectrum to that of WT, it is obvious that the 1691- cm^{-1} band corresponding to the P_L C_9 keto carbonyl is not present (see Figure 2A). In addition, the carbonyl stretching frequency region is congested and unresolved. Spectral deconvolution indicates that there are components centered at 1673 and 1684 cm^{-1} . Simply subtracting the WT spectrum from that of the mutant demonstrates that there is a positive component at ca. 1670 cm^{-1} and a negative component at 1694 cm^{-1} (data not shown). The negative band is indicating the absence of the 1691- cm^{-1} band of the P^0 WT spectrum corresponding to the keto carbonyl of P_L . The simplest interpretation of the positive band at ca. 1670 cm^{-1} is that it corresponds to the 1691 cm^{-1} band in the WT P^0 spectrum that has downshifted to 1673 cm^{-1} (Figure 2A). This would indicate that the 1691- cm^{-1} band downshifts ~ 18 cm^{-1} , consistent with the formation of a new hydrogen bond on the C_9 keto carbonyl of P_L . The 1684- cm^{-1} band reflects a modest perturbation of the P_M keto carbonyl. Also present in this P^0 spectrum is a 1627- cm^{-1} band which has upshifted compared to that of WT at 1620 cm^{-1} , indicating a weakened hydrogen bond.

D9 Double LH(M160) + LH(L131) Mutant. With respect to WT, changes in the FT Raman spectrum of P^0 from the D9 double mutant appear essentially as the additive contributions of changes seen in the spectra from the individual mutants. There is a conspicuous absence of intensity in the entire 1680–1690- cm^{-1} spectral region while in the congested region from 1650 to 1680 cm^{-1} there appears to be present two maxima at 1657 and 1673 cm^{-1} (Figure 2A) which match the new bands observed for the LH(M160) and LH(L131)

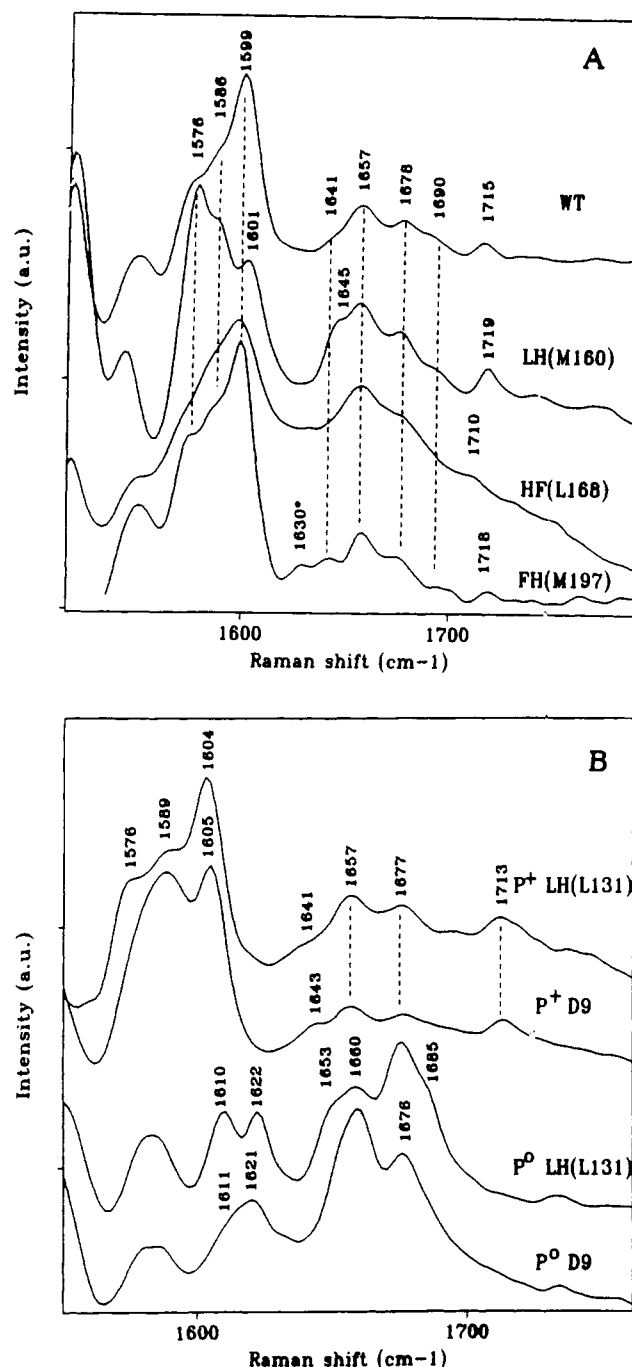


FIGURE 3: (A) Room temperature P^+ FT resonance Raman spectra of wild-type and mutant RCs from *Rb. sphaeroides*. RCs were poised in their P^+ state with ferricyanide. Same experimental conditions as in Figure 2. (B) Low temperature (15 K) P^+ FT resonance Raman spectra of wild-type and the LH(L131) and D9 double LH(L131)+LH(M160) mutants. The P^+ states were obtained by rapid freezing under continuous illumination.

mutants, respectively. Thus, the effects of each individual mutation is conserved in the D9 mutant, that is, the change in hydrogen bond interactions of both keto carbonyls of P , as well as the secondary-effect perturbation on the C_2 P_L acetyl carbonyl band at 1627 cm^{-1} . Therefore, the FT Raman data of the D9 double mutant, in conjunction with the LH(M160) and LH(L131) mutant P^0 spectra, indicate that the single and double mutations have, indeed, introduced new hydrogen bonds to the keto carbonyls, as designed, and the FT Raman spectra reflect these changes in complete accordance with our model. Furthermore, since the observed downshifts of the P_M (-22 cm^{-1}) and P_L (-18 cm^{-1}) keto carbonyl stretching modes

are similar, the genetically introduced hydrogen bonds are of similar strengths.

FH(M197) Mutant. Figure 2B shows the FT Raman spectrum of the FH(M197) mutant that has been designed to introduce a new hydrogen bond to the free C₂ acetyl carbonyl of P_M. This spectrum shows the appearance of a new band at 1630 cm⁻¹ and the disappearance of the 1653-cm⁻¹ band that has been assigned as arising from the free acetyl carbonyl of P_M. These observations are totally consistent with the formation of a new hydrogen bond to the C₂ acetyl carbonyl of P_M with the 1653-cm⁻¹ band downshifting to 1630 cm⁻¹. The band at 1660 cm⁻¹, as we have previously stated (see above), does not arise from P^o (Mattioli *et al.*, 1991). Recently we have reported the FT Raman spectrum of a similar mutant at the same residue, M197 (Wachtveitl *et al.*, 1993), where a tyrosine residue, instead of a histidine residue, has replaced the phenylalanine M197. The spectra of these two mutants are virtually identical except the resulting hydrogen bond in the FY(M197) mutant downshifts less, only to 1636 cm⁻¹. The larger shift for the FH(M197) mutant reported here reflects a stronger hydrogen bond.

HF(L168) Mutant. This mutation was designed to remove an existing hydrogen bond on the C₂ acetyl carbonyl of P_L. Figure 2B shows that the 1620-cm⁻¹ band assigned to this acetyl carbonyl vibration is completely absent in the HF-(L168) P^o spectrum. Comparing this spectrum with that of WT, there is additional intensity under the 1653-cm⁻¹ band; this is readily seen in a difference spectrum with WT where a positive component appears at ca. 1645 cm⁻¹ (data not shown). This is interpreted as the upshift of the 1620-cm⁻¹ band to ca. 1653 cm⁻¹, consistent with the breaking of the hydrogen bond from His L168 to the C₂ acetyl carbonyl of P_L. Spectral deconvolution of the P^o spectrum of this mutant does not reveal a component at 1645 cm⁻¹ nor two components near 1653 cm⁻¹, thus we estimate the frequency of the band corresponding to the P_L acetyl to be at ca. 1653 cm⁻¹ for this mutant. There are also some minor structural changes associated with this mutation as is seen by a modest perturbation of the stretching frequency of the P_L keto carbonyl that is present as a shoulder at 1688 cm⁻¹. The disappearance of the 1620-cm⁻¹ band in the FT Raman spectrum of the HF(L168) mutant is compelling evidence that this band is attributable to the C₂ acetyl carbonyl of P_L and that it does not arise from possible C_aC_m or C_bC_b stretching modes that could be expected to be observed in the 1620–1650-cm⁻¹ region (Donohoe *et al.*, 1988).

Fourier Transform Resonance Raman Spectrum of P⁺

Structurally informative new bands arising from P⁺ formation appear in the FTRR spectrum of oxidized WT RCs at 1600, 1641, and 1717 cm⁻¹. These bands arise, respectively, from the downshift of the 1607 cm⁻¹ (corresponding to C_aC_m stretching mode) and the upshift of the 1620 (C₂ acetyl carbonyl) and the 1691 cm⁻¹ (C₉ keto carbonyl) of P (Mattioli *et al.*, 1991). The trends of these shifts are totally consistent with the one-electron oxidation of a molecule possessing a redox orbital of A_{1u}-like character (Oertling *et al.*, 1987), such as the case for BChl *a*. The magnitude of the oxidation-induced upshift of 26 cm⁻¹ of the P carbonyl band from 1691 to 1717 cm⁻¹, as compared to that of monomeric BChl *a* in nonprotic solvents (+32 cm⁻¹; Mäntele *et al.*, 1988; cf. Heald & Cotton, 1990) indicates that the resulting positive charge following the oxidation of P is not equally shared but primarily resides on one of the two BChl *a* molecules constituting P. From the appearance of a 1641-cm⁻¹ band in the P⁺ FT RR

Table 2: Observed Upshift (in cm⁻¹) in the C₉ Keto Carbonyl of P_L upon P⁺ Formation^a

	P	P ⁺	Δ	%P _L ⁺
WT	1691–2 ^b	1715	23–24	72–75
LH(M160)	1693–4 ^b	1719	25–26	78–81
LH(L131) ^c	1677	1713	36	
D9 ^c	1677	1713	36	
FH(M197)	1693	1717	24	75
HF(L168)	1688	1710	22	68

^a Localization of the unpaired electron spin density on the P_L component is identified by the presence of a ca. 1641-cm⁻¹ band assigned to P_L in the FTRR spectrum of P⁺ in the mutant RCs. ^b These values are reported, in the table and throughout the text, as observed directly from the Raman spectra and as observed in their deconvolved spectra; they are seen to differ by 1 cm⁻¹, which corresponds to the instrumental error. ^c Spectra measured at 15 K.

spectrum, it was identified that the positive charge resides mainly on P_L; assuming a +32-cm⁻¹ upshift observed *in vitro* represents 100% localization, the localization on P_L was estimated at ca. 80% (Mattioli *et al.*, 1991). Interestingly, a similar value for one or the other of the two BChls of P was calculated by Parson *et al.* (1992) for *Rps. viridis*. ENDOR/TRIPLE studies (Rautter *et al.*, 1992) on *Rb. sphaeroides* RCs have also concluded that the majority of the unpaired spin density is on P_L, but the estimate of ca. 68% is somewhat lower than what is estimated by the FT RR data (see Discussion).

In the following, we estimate the degree of localization of the unpaired electron spin density (or resulting positive charge) on P_L in the P⁺ state of the mutants based on the observed upshift of the P_L keto carbonyl upon oxidation to the P⁺ state, and relate this upshift to that observed *in vitro* for the one-electron oxidation of BChl *a*⁺ (+32 cm⁻¹); these estimates are based on the simple assumption that the upshift is proportional to the charge localization (Bradley *et al.*, 1981; Angel *et al.*, 1984; Duchowski & Bocian, 1990) and that +32 cm⁻¹ represents 100% localization (Mattioli *et al.*, 1991). The error of the reported band positions is 1 cm⁻¹ which translates to an error of 3% in our estimation; the observed trends of increase or decrease should be qualitatively correct. The upshift of the keto carbonyl should be a more reliable marker than the acetyl carbonyl to gauge the degree of localization because the latter could suffer from conformational changes upon oxidation which would affect its observed vibrational frequency. However, the presence of a 1640–1645-cm⁻¹ band in the P⁺ spectrum identifies the (partially) oxidized P_L species in P⁺ (see Table 2).

Wild Type. The *Rb. sphaeroides* wild-type P⁺ room temperature FT RR spectrum (Figure 3A) of the WT RCs studied in this work is essentially the same as those from R 26 and another 2.4.1 strain (Mattioli *et al.*, 1991, 1992a; Wachtveitl *et al.*, 1993). Comparing these spectra, the P⁺ spectrum from the WT RCs has a small but significant difference between the vibrational frequency of the free C₉ keto carbonyl compared to that already reported. This band is seen at 1715 cm⁻¹ for the WT RC preparation reported here and not at 1717 cm⁻¹ (Mattioli *et al.*, 1991, 1993; Wachtveitl *et al.*, 1993); considering it has upshifted from 1691–1692 cm⁻¹ (see Table 2) in the neutral species to 1715 cm⁻¹, this represents a 23–24-cm⁻¹ (72–75% positive charge localization on P_L) upshift instead of 26 cm⁻¹ (81% on P_L). Thus, for the WT strain reported here, the estimated localization of the positive charge on P_L is less than that for R 26 and 2.4.1 strains and is closer to that estimated by ENDOR measurements (68% on P_L) on the same WT strain (Rautter *et al.*, 1992). The origin for this lower upshift in the C₉ keto carbonyl

and decreased localization on P_L is not known. It could result from the particular lab strain or its particular growth conditions. Work to date in our laboratory comparing FT RR spectra of WT and mutant RCs solubilized and in chromatophores suggests that this difference should not be due to detergent or RC solubilization.

LH(M160) Mutant. The room temperature FTRR spectrum of P^+ of the LH(M160) mutant displays a 1645- and a 1719- cm^{-1} band (Figure 3A) which are both slightly higher in frequency than their corresponding counterparts in the WT spectrum (1642 and 1715 cm^{-1} , respectively). These bands indicate that the positive charge is still predominantly localized on P_L ; however, it appears to be more so in this mutant. For wild-type $P \rightarrow P^+$ oxidation resulted in a 1620 to 1641 $\text{cm}^{-1} = 21 \text{ cm}^{-1}$ and a 1691–1692 to 1715 $\text{cm}^{-1} = 24\text{--}23 \text{ cm}^{-1}$ upshift of the C_2 and C_9 carbonyls, respectively, while for the LH-(M160) mutant we observe the shifts 1618 to 1645 $\text{cm}^{-1} = 27 \text{ cm}^{-1}$ and 1693–1694 to 1719 $\text{cm}^{-1} = 26\text{--}25 \text{ cm}^{-1}$ for the C_2 and C_9 carbonyls, respectively (see Table 2). Using the shift of the C_9 keto carbonyl as a gauge of the extent of electron localization, it appears that ca. 78–81% of the spin density is on P_L in the mutant compared to 72–75% for WT. An increase in positive charge localization on P_L for this mutant has also been concluded by Rautter *et al.* (1992) from ENDOR measurements consistent with our conclusions. Furthermore, it is noted that in Figure 3A the relative intensities of the 1576-, 1586-, 1645-, and 1717- cm^{-1} bands with respect to that at 1599 cm^{-1} are more intense compared to those of the WT P^+ spectrum. Similar features in intensity pattern and band shifts were observed in a FY(M197) mutant of *Rb. sphaeroides* in which the positive charge localization on P_L in P^+ was concluded (Wachtveitl *et al.*, 1993). This intensity pattern change indicates a change in the resonance condition at 1064 nm giving rise to the resonance Raman spectrum of P^+ in this mutant compared to WT.

HF(L168) Mutant. In the room temperature P^+ FTRR spectrum (Figure 3A) of this mutant there is no observable band at ca. 1640 cm^{-1} ; this is entirely consistent with our assignments since it arises from the upshift of a 1620- cm^{-1} band that is not present in the P^0 spectrum. In the C_9 keto carbonyl region there is a weak band at 1710 cm^{-1} which is unusually lower in frequency than that observed in WT or any of the other mutants. Assuming this band has upshifted from the 1688- cm^{-1} component in the P^0 spectrum of this mutant, this would correspond to a 22 cm^{-1} upshift of the C_9 keto carbonyl band, giving an estimated ca. 68% localization of the unpaired spin density on P_L . Another way of interpreting these data is that the 1710- cm^{-1} band arises from the shift of the 1680- cm^{-1} band of the P_M keto carbonyl. In this interpretation the keto frequency has upshifted by 30 cm^{-1} and would indicate that the spin density is nearly totally localized on P_M , estimated to be ca. 94%. In view of the absorption spectrum of P^+ in the near-IR region (data not shown), we do not favor a nearly "monomeric" P^+ species with the positive charge almost entirely on P_M . In either case, the removal of the His L168 which forms a strong hydrogen bond on the C_2 acetyl carbonyl of P_L results in a significant decrease in the unpaired spin density on P_L in the P^+ state toward a more symmetrically distributed situation. This mutant shows a significant decrease in relative intensity of the 1576-, 1586-, and 1710- cm^{-1} bands with respect to the 1599- cm^{-1} band as compared to the WT P^+ spectrum, a trend which is opposite to what is observed for the LH(M160) mutant. This intensity pattern has also been observed in the MT(L248) and SG(L244) mutant RCs from *Rb. sphaeroides*

where it was concluded that the positive charge localization on P_L had decreased for both these mutants (Wachtveitl *et al.*, 1993).

FH(M197) Mutant. The room temperature P^+ FTRR spectrum of the FH(M197) mutant is shown in Figure 3A; because of the higher P/P^+ redox midpoint potential of this mutant (125 mV above that of WT; Williams *et al.*, unpublished results) ferricyanide addition did not result in the complete oxidation of P , and thus the neutral P^0 contributions (ca. 40% weighting) were subtracted from the P^+ spectrum. This resulting spectrum exhibits a weak 1718- cm^{-1} (see Figure 3A) band which has upshifted from 1693 cm^{-1} indicating that the positive charge localization (estimated to be ca. 75% on P_L) is similar to that of WT. Because we could not fully oxidize the primary donor in this case, we stably trapped P^+ by illuminating at room temperature and quickly froze the RC sample while still illuminated. This resulted in a greater population of P^+ . We confirmed that the 1718- cm^{-1} band was still present at 15 K (data not shown); the frequency position of this band is not expected to shift upon the freezing technique we employ [see, for example, Mattioli *et al.* (1992b)].

LH(L131) and D9 Double LH(M160) + LH(L131) Mutants. Because these two mutants are in hydrogen bonding interaction at the C_9 keto carbonyl group with the genetically introduced His L131 residue, it is difficult to reliably estimate the degree of positive charge localization on P_L . For example, the upshift of the C_9 keto carbonyl upon P oxidation will be affected by possible changes in hydrogen bond strength. The 15 K FT Raman spectra of these two mutants in their P^+ states (see Figure 3B) exhibit a 1713- cm^{-1} band; the frequency position of this band for WT and the FH(M197) mutant (data not shown) does not shift upon use of the freezing technique we employ [see, for example, Mattioli *et al.* (1992b)]. Also present in the spectra are bands at 1641 and 1643 cm^{-1} for the LH(L131) and D9 double mutant, respectively, which may be indicating that the positive charge is more localized on P_L for the D9 double mutant compared to the LH(L131) mutant. This interpretation is in agreement with those of the ENDOR measurements (Rautter *et al.*, 1992) but because the 1713- cm^{-1} band of the P_L keto is not significantly different for both these mutants, our assessment is not corroborated.

DISCUSSION

The FT Raman study reported here fully confirms (i) the formation of hydrogen bonds on the C_9 keto carbonyls of the primary donor in *Rb. sphaeroides* mutants designed to introduce such hydrogen bonds (Williams *et al.*, 1992), consistent with the conclusions from FTIR difference studies on chromatophores (Nabedryk *et al.*, 1993); however, the FTIR studies found a stronger hydrogen bond than that reported for the LH(L131) mutant; (ii) the formation of a hydrogen bond with the C_2 acetyl carbonyl of P_M in the FH-(M197) mutation and the removal of the hydrogen bond to the P_L C_2 acetyl carbonyl in the HF(L168) mutation.

Unpaired Electron Spin Density Localization. The results presented indicate that hydrogen bonds (on the order of 0.10–0.20 eV in bond enthalpy, see below), donated by histidine residues, to the primary donor can significantly alter the positive charge localization in the oxidized dimer. For *Rb. sphaeroides*, the unpaired spin density in the primary donor in the P^+ state has been suggested by experiment to be residing asymmetrically [for a review, see Lubitz (1991)] in favor of P_L (Mattioli *et al.*, 1991; Rautter *et al.*, 1992). This localization should arise from an energetic difference in the

P_L and P_M molecular orbitals constituting the dimer redox orbital. The situation where the resulting positive charge resides mainly on P_L indicates that the redox orbital of P from which the electron is removed possesses significant P_L HOMO character, and that this P_L HOMO is higher in energy than that of P_M by 0.11–0.14 eV according to a recent model (Rautter *et al.*, 1992; Plato *et al.*, 1992); this energy difference is similar in magnitude to the hydrogen bond enthalpies found in this work (see below).

Table 2 lists the changes in P_L^+ localization as deduced from the FT Raman measurements. For the M160 mutant, we observe an increase in the localization of the positive charge on P_L . In the above model, this observation may be rationalized as a stabilization of the P_M molecule via this newly introduced hydrogen bond which increases the energy difference between P_L and P_M thus localizing even more the positive charge on P_L . Similar conclusions were reported by Rautter *et al.* (1992). In the same way of thinking, if a hydrogen bond is broken on the P_L molecule, then one would expect that the P_L energy will increase and the P_M and P_L energies to be more different and thus the positive charge be more localized on P_L as well. This seems not to be the case for the HF(L168) mutation (see Table 2) where the hydrogen bond between His L168 and the C_2 acetyl carbonyl of P_L has been removed. However, the formation of a new hydrogen bond on the P_M acetyl carbonyl in the FH(M197) mutant does not appear to change the degree of localization. In contrast, the FY(M197) mutation (Wachtveitl *et al.*, 1993) showed a significant increase in the localization on P_L . These results indicate that the predicted effects of the formation of a hydrogen bond on the acetyl carbonyls of P, according to the above model, may be subject to other factors. For example, these hydrogen bonds to the acetyl carbonyls may alter their angle with the plane of the macrocycle, thus affecting the resulting spin density distributions. Another factor to be considered for these mutants is the modified protein electrostatic interactions with P_M^+ or P_L^+ which may destabilize charge localization on one or the other. The possibility that the distance between P_L and P_M has changed seems unlikely since neither the P^*/P optical band nor the P^* fluorescence has changed significantly (Williams *et al.*, unpublished results).

Redox Properties of P. It is interesting to compare the FH(M197) mutant studies here with the FY(M197) mutant reported elsewhere (Wachtveitl *et al.*, 1993). Both mutations resulted in the formation of a new hydrogen bond with the C_2 acetyl carbonyl of P_M , but with His and Tyr residues, respectively. As seen in the FT Raman spectra, the observed frequency of the C_2 acetyl carbonyl stretching mode of the His-donated hydrogen bond (1630 cm^{-1}) is lower than that corresponding to the Tyr-donated hydrogen bond (1636 cm^{-1}). In principle, this indicates that the His-donated hydrogen bond in the FH(M197) mutant RC is stronger than the Tyr-donated hydrogen bond in the FY(M197) mutant RC. We may estimate the hydrogen bond enthalpies which correspond to these observed carbonyl frequency downshifts by using the empirical Badger-type empirical relations as given in Zadorozhnyi and Ishchenko (1965). If we take 1653 cm^{-1} to represent the vibrational frequency of a BChl a C_2 acetyl carbonyl stretching mode, free of intermolecular interaction, then the 1630-cm^{-1} frequency observed for this mode in the FH (M197) Raman spectrum would correspond to an estimated bond enthalpy of 0.145 eV (Table 1). For the FY-(M197) mutant (Wachtveitl *et al.*, 1993), the 1636-cm^{-1} band would correspond to a hydrogen bond enthalpy of only 0.114 eV. It is noted that both these bond enthalpy values are

significantly lower than that for the hydrogen bond in WT between the P_L C_2 acetyl carbonyl (vibrating at 1620 cm^{-1}) and His L168; this bond enthalpy would be estimated at 0.207 eV. We stress that these enthalpy values are estimates, but it is useful to consider the relative energetics of the hydrogen bonds formed in the mutants with respect to WT. The very strong hydrogen bond at the C_2 acetyl carbonyl with His L168, as reflected by the low frequency of 1620 cm^{-1} , is observed in the FT Raman spectra of *Rb. sphaeroides*, *Rhodobacter capsulatus*, and *Rhodospirillum rubrum* (Mattioli *et al.*, 1992a), three species in which His L168 is conserved (Komiya *et al.*, 1988). The stronger hydrogen bond of the FH(M197) mutant as compared to the FY(M197) mutant could be due to a more favorable hydrogen bond geometry in the former mutant or it could be due to the chemical nature of the hydrogen bond donor, or a combination of both. The dipole moment of imidazole (ca. 4 debye, Grimmett, 1970) is considerably greater than that of phenol (1.45 debye) and could explain the histidine hydrogen bond being stronger than a tyrosine hydrogen bond even if geometry changes were not a factor.

Another difference between the two mutations at M197 is the interesting observation that the Phe \rightarrow His mutation results in the increase of ca. 125 mV in the P/P^+ redox midpoint potential whereas, in the Phe \rightarrow Tyr mutation, the P/P^+ potential increases by only ca. +20 mV (Wachtveitl *et al.*, 1993). In principle, the formation of hydrogen bonds on the conjugated carbonyls of P should preferentially stabilize the neutral ground state of P and thus raise the P/P^+ redox midpoint potential (Williams *et al.*, 1992a). One reason for this significant difference in oxidation potentials could be that the hydrogen bond to the P_M acetyl carbonyl is stronger in the FH(M197) mutant than in the FY(M197) mutant. However, if this is the sole reason, then the effect is not a linear one; the increase in redox potential of the FH(M197) mutation is 6 times that of the FY(M197) while the estimated bond enthalpies differ by a factor of only 1.3. It seems that the strength of the hydrogen bond formed on P may not be the sole reason governing the increase in the P/P^+ midpoint potential. Furthermore, each new histidine hydrogen bond formed with the C_2 or C_9 carbonyls of P independently increases the P oxidation potential in an additive fashion, as seen for the D9 double mutant (Williams *et al.*, 1992b). This additivity correlates with the additivity of the formed hydrogen bonds for this mutant (Figure 2A).

CONCLUSIONS

We have identified all the C_2 and C_9 carbonyl vibrators of P in *Rb. sphaeroides* (Mattioli *et al.*, 1991). These hydrogen bonds are of sufficient energy as to influence the degree of positive charge localization in the P^+ . The addition of hydrogen bonds, with histidine as the donor, to the conjugated carbonyl groups of P appears to systematically result in an increase in P/P^+ redox midpoint potential by 60–120 mV. As well, the removal of a conserved hydrogen bond to the P_L acetyl carbonyl, donated by histidine L168, results in an 80 mV decrease of the P/P^+ redox potential. This significant change in redox potential is not observed in a *Rb. sphaeroides* mutant where a new hydrogen bond on an acetyl carbonyl of P is donated by tyrosine (Wachtveitl *et al.*, 1993). These results suggest that the chemical nature of the hydrogen bond donor to the conjugated carbonyls of P plays a significant role in modifying its redox properties.

ACKNOWLEDGMENT

We thank Dr. Marc Lutz for helpful discussions.

REFERENCES

- Allen, J. P., Feher, G., Yeates, T. O., Komiya, H., & Rees, D. C. (1987) *Proc. Natl. Acad. Sci. U.S.A.* **84**, 5730–5734.
- Angel, S. M., DeArmond, M. K., Donohoe, R. J., Hanck, K. W., & Wertz, D. W. (1984) *J. Am. Chem. Soc.* **106**, 3688–3689.
- Bradley, P. G., Kress, N., Hornberger, B. A., Dallinger, R. F., & Woodruff, W. H. (1981) *J. Am. Chem. Soc.* **103**, 7441–7446.
- Chirino, A. J., Lous, E. J., Huber, M., Allen, J. P., Schenck, C. C., Paddock, M. L., Feher, G., & Rees, D. C. (1994) *Biochemistry* (submitted).
- Donohoe, R. J., Frank, H. A., & Bocian, D. F. (1988) *Photochem. Photobiol.* **48**, 531–537.
- Donohoe, R. J., Dyer, R. B., Swanson, B. I., Violette, C. A., Frank, H. A., & Bocian, D. F. (1990) *J. Am. Chem. Soc.* **112**, 6716–6718.
- Duchowski, J. K., & Bocian, D. F. (1990) *Inorg. Chem.* **29**, 4158–4160.
- El-Kabbani, O., Chang, C.-H., Tiede, D., Norris, J., & Schiffer, M. (1991) *Biochemistry* **30**, 5361–5369.
- Ermiler, U., Fritzsche, G., Buchanan, S., & Michel, H. (1992) in *Research in Photosynthesis* (Murata, N., Ed.) Vol. I, pp 341–347, Kluwer Academic, The Netherlands.
- Grimmett, M. R. (1970) *Adv. Heterocycl. Chem.* **12**, 103–183.
- Heald, R. L., & Cotton, T. M. (1990) *J. Phys. Chem.* **94**, 3968–3975.
- Holzappel, W., Finkle, U., Kaiser, W., Oesterhelt, D., Scheer, H., Stiltz, H. U., & Zinth, W. (1990) *Proc. Natl. Acad. Sci. U.S.A.* **87**, 5168–5172.
- Kirmaier, C., Holten, D., & Parson, W. W. (1985) *Biochim. Biophys. Acta* **810**, 49–61.
- Komiya, H., Yeates, T. O., Rees, D. C., Allen, J. P., & Feher, G. (1988) *Proc. Natl. Acad. Sci. U.S.A.* **85**, 9012–9016.
- Krawczyk, S. (1989) *Biochim. Biophys. Acta* **976**, 140–149.
- Lendzian, F., Endeward, B., Plato, M., Bumann, D., Lubitz, W., & Möbius, K. (1990) in *Reaction Centers of Photosynthetic Bacteria* (Michel-Beyerle, M.-E., Ed.) pp 57–68, Springer-Verlag, Berlin.
- Lubitz, W. (1991) in *The Chlorophylls* (Scheer, H., Ed.) pp 903–944, CRC Press, Boca Raton, FL.
- Lutz, M. (1984) in *Advances in Infrared and Raman Spectroscopy* (Clark, R. J. H., & Hester, R. E., Eds.) Vol. 11, pp 211–300, Wiley, New York.
- Lutz, M., & Robert, B. (1988) in *Biological Applications of Raman Spectroscopy* (Spiro, T. G., Ed.) Vol. 3, pp 347–411, Wiley-Interscience, New York.
- Lutz, M., & Mantele, W. (1991) in *Chlorophylls* (Scheer, H., Ed.) pp 855–902, CRC Press, Boca Raton, FL.
- Mantele, W. G., Wollenweber, A. M., Nabedryk, E., & Breton, J. (1988) *Proc. Natl. Acad. Sci. U.S.A.* **85**, 8468–8472.
- Martin, J.-L., Breton, J., Hoff, A., & Antonetti, A. (1986) *Proc. Natl. Acad. Sci. U.S.A.* **83**, 957–961.
- Mattioli, T. A., Hoffmann, A., Robert, B., Schrader, B., & Lutz, M. (1991) *Biochemistry* **30**, 4648–4654.
- Mattioli, T. A., Robert, B., & Lutz, M. (1992a) in *The Photosynthetic Bacterial Reaction Center: Structure, Spectroscopy, and Dynamics* (Breton, J., & Vermeiglio, A., Eds.) pp 127–132, Plenum, New York.
- Mattioli, T. A., Sockalingum, D., Lutz, M., & Robert, B. (1992b) in *Research in Photosynthesis* (Murata, N., Ed.) Vol. I, pp 405–408, Kluwer, Dordrecht, The Netherlands.
- Mattioli, T. A., Hoffmann, A., Sockalingum, D. G., Schrader, B., Robert, B., & Lutz, M. (1993) *Spectrochim. Acta* **49A**, 785–799.
- Michel, H., Epp, O., & Deisenhofer, J. (1986) *EMBO J.* **5**, 2445–2451.
- Morita, E. H., Hayashi, H., & Tasumi, M. (1993) *Biochim. Biophys. Acta* **1142**, 146–154.
- Murchison, H. A., Alden, R. G., Allen, J. P., Peloquin, J. M., Taguchi, A. K. W., Woodbury, N. W., & Williams, J. C. (1993) *Biochemistry* **32**, 3498–3505.
- Nabedryk, E., Allen, J. P., Taguchi, A. K. W., Williams, J. C., Woodbury, N. W., & Breton, J. (1993) *Biochemistry* **32**, 13879–13885.
- Oertling, W. A., Salehi, A., Chung, Y. C., Leroi, G. E., Chang, C. K., & Babcock, G. T. (1987) *J. Phys. Chem.* **91**, 5887–5898.
- Palaniappan, V., Aldema, M. A., Frank, H. A., & Bocian, D. F. (1992) *Biochemistry* **31**, 11050–11058.
- Parson, W. W., Nabedryk, E., & Breton, J. (1992) in *The Photosynthetic Bacterial Reaction Center: Structure, Spectroscopy, and Dynamics* (Breton, J., & Vermeiglio, A., Eds.) pp 79–88, Plenum, New York.
- Plato, M., Lendzian, F., Lubitz, W., & Möbius, K. (1992) in *The Photosynthetic Bacterial Reaction Center: Structure, Spectroscopy, and Dynamics* (Breton, J., & Vermeiglio, A., Eds.) pp 109–118, Plenum, New York.
- Rautter, J., Gessner, Ch., Lendzian, F., Lubitz, W., Williams, J. C., Murchison, H. A., Wang, S., Woodbury, N. W., & Allen, J. P. (1992) in *The Photosynthetic Bacterial Reaction Center: Structure, Spectroscopy, and Dynamics* (Breton, J., & Vermeiglio, A., Eds.) pp 99–108, Plenum, New York.
- Robert, B. (1990) *Biochim. Biophys. Acta* **1017**, 99–111.
- Shreve, A. P., Cherepy, N. J., Franzen, S., Boxer, S. G., & Mathies, R. A. (1991) *Proc. Natl. Acad. Sci. U.S.A.* **88**, 11207–11211.
- Wachtveitl, J., Farchaus, J. W., Dos, R., Lutz, M., Robert, B., & Mattioli, T. A. (1993) *Biochemistry* **32**, 12875–12886.
- Williams, J. C., Alden, R. G., Peloquin, J. M., Woodbury, N. W., & Allen, J. P. (1992a) *Biochemistry* **31**, 11029–11037.
- Williams, J. C., Alden, R. G., Coryell, V. H., Lin, X., Murchison, H. A., Peloquin, J. M., Woodbury, N. W., & Allen, J. P. (1992b) in *Research in Photosynthesis* (Murata, N., Ed.) Vol. I, pp 377–380, Kluwer, Dordrecht, The Netherlands.
- Woodbury, N. W., Becker, M., Middendorf, D., & Parson, W. W. (1985) *Biochemistry* **24**, 7516–7521.
- Yeates, T. O., Komiya, H., Chirino, A., Rees, D. C., Allen, J. P., & Feher, G. (1988) *Proc. Natl. Acad. Sci. U.S.A.* **85**, 7993–7997.
- Zadorozhnyi, B. A., & Ishchenko, I. K. (1965) *Opt. Spectrosc. (Engl. Transl.)* **19**, 306–308.